Workshop on Visualisation in Environmental Sciences (EnvirVis) (2017)
R. Bujack and A. Middel and K. Rink and D. Zeckzer (Editors)

Video Compression for Ocean Simulation Image Databases

Anne S. Berres[1], Terece L. Turton[2], Mark Petersen[1], David H. Rogers[1], and James P. Ahrens[1]

[1] Los Alamos National Laboratory, Los Alamos, NM, USA
[2] Center for Agile Technology, University of Texas at Austin, TX, USA

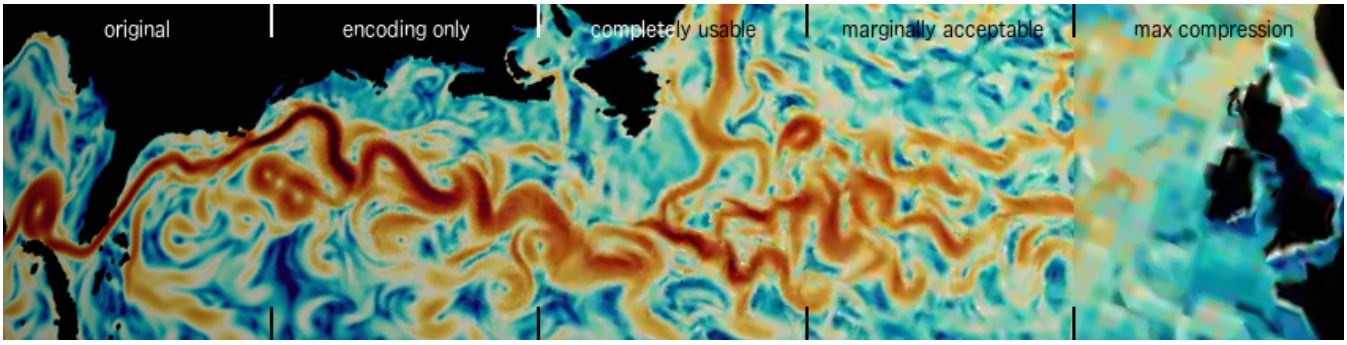

Figure 1: *Progression of video compression results for kinetic energy. From left to right: original quality, encoding only, completely usable (CRF=30), marginally acceptable (CRF=34), and maximal compression (CRF=51). Encoding alone and CRF=30 are nearly indistinguishable from the original, CRF=34 is more noticeable, and maximal compression washes out most features.*

Abstract

Climate research requires monitoring a large range of spatial and temporal scales to understand the climate system and potential future impacts. Climate simulations are now run with very high resolution (1–10 km gridcells) ocean, sea ice, and atmosphere components, and can easily produce petabytes of output. This overloads storage systems and hinders visualization and analysis. Image databases can decrease storage sizes from petabytes of simulation output down to several hundred gigabytes of images.

In this paper, we introduce video compression as a method to further decrease database sizes by 2-4 orders of magnitude. We compare compression and access speeds, compressed sizes, and compression quality over a range of settings. Quality is assessed through image quality metrics and expert feedback. Overall, we were able to show that video compression techniques provide an efficient means of storing image databases at a shareable size, while preserving image quality. This enables the wise use of available disk space, so scientists can more easily study the physical features of interest.

Categories and Subject Descriptors (according to ACM CCS): Data Storage Representations [E.2.5]: Data Representation—; Image Processing and Computer Vision [I.4.2]: Compression (Coding)—

1. Motivation

Increasing supercomputer speeds have led to higher spatial resolution in global climate models, from 100 km gridcells in past years to 1–10 km today. This is motivated by an improved representation of physical processes, e.g. cloud-resolving scales in the atmosphere and eddy-resolving in the ocean. Eddies occur at scales of 10–30 km and smaller, but are responsible for transport of heat and nutrients that impact the large scales [SPA*15]. There is evidence that eddies in the Southern Ocean impact the meridional overturning circulation in the North Atlantic [MJM13]. As model resolutions proceed to these high resolutions, scientists struggle to visualize, analyze, and archive large volumes of data, and must look at the other fields for innovative solutions to this problem [WPS*16].

There is a large body of work on compressing and sampling different kinds of data, ranging from compression of unstructured floating point data [Lin14, LI06] to adaptive refinement [NWP*14] and multi-resolution approaches [LJ14]. In addition, there have been numerous approaches to visualizing and interacting with these large datasets, ranging from in-situ processing and combining in-situ and in-transit processing [BAB*12], to query-driven computations and remote rendering [ASW12, GABJ08], and tracking differences over time [WCBP12]. Ayachit

DOI: 10.2312/envirvis.20171104

et al. [ABG*15] presented ParaView Catalyst, a library that enables in-situ processing, analysis, and visualization that integrates with VTK [MOD15] and ParaView [FMT*11]. Ahrens et al. introduced image databases [AJO*14] containing large numbers of visualization images. Images are generated in-situ using Catalyst, and users can interactively explore image databases as if they were interacting with the data directly, using a Cinema Viewer [Dat17]. Using image databases, the data volume can be reduced from an order of petabytes to an order of terabytes. While this makes it easier to interact with the dataset, sharing is still a challenge, as even a very small dataset can easily exceed 1 GB. Traditional image compression techniques, such as wavelet compression [GS01, WMB*11] can reduce image sizes by a linear factor. Exploiting spatial and temporal coherence can aid in compressing image databases to a sharable size. Ellsworth et al. [EGH*06] encode camera streams using MPEG-1 to achieve a compression of 17 % on disk. Kageyama et al. [KY14] have adapted this approach for in-situ visualization with a compression of 14 %. Fernandez et al. [FFSE14] exploit spatial coherence within volumetric depth images to compress them, achieving compression rates of 0.07 % – 36.06 % with varying error. Sohn et al. [SBS04] present a block-based wavelet transform with temporal encoding for volumetric data, which exploits empty space, achieving compression rates of 0.29 % – 0.68 %.

In this work, we propose a workflow, visually represented by Figure 2, through which image databases can be compressed by 2-4 orders of magnitude with varying perceptual loss, and which allows for efficient arbitrary access to individual images. We compare databases from all steps of the workflow and across the entire range of encoding and compression parameters. To evaluate the success of our method, we consider compression and access speeds, compressed size, as well as image quality metrics and expert feedback. The contribution of this workflow is:

- Optimization of multi-dimensional climate dataset traversal.
- Quasi-lossless and lossy compression of climate data to a much smaller size than previous works.
- Quantitative and perceptual evaluation of the resulting imagery.

2. Video Compression for Image Databases

The most significant advantage of video compression techniques is their efficient compression of sequences of similar images. In a movie, the background stays the same for several frames in a row. Video compression exploits these similarities to efficiently compress tens of thousands of images into a single, much smaller file.

Ocean data is uniquely poised to take advantage of video compression techniques. With optimal cropping (globe rendered to a square image), about 21.5 % of each image is background. With 71 % of the earth covered with water, this results in an average of 56 % of pixels per image that contain ocean information. If they are put in a coherent order, ocean image databases compress extremely well with video compression.

We compress simulation data from a run of the Model for Prediction Across Scales - Ocean (MPAS-Ocean), a multi-resolution approach to ocean modeling with a wide array of variables of interest to the scientist. This simulation is part of the Accelerated Climate Model for Energy (ACME), a project to develop leading-edge climate and earth models [MM05, MPA, RPH*13]. The simulation run we used has 173 time steps at 5 day intervals, and multi-resolution grid with 30km cells at the equator and 10km cells at the poles, resulting in a total of ca. 3 mio cells in a 20.47 GB NetCDF file.

2.1. Traversing Image Databases

From this simulation run, we generated an image database with four dimensions: time, variables, and two parametrized camera angles φ, ϑ. We chose three variables of interest to climate scientists: salinity (SA), temperature (TE), and kinetic energy (KE), and rendered them with different colormaps to examine compression performance under a variety of conditions. To facilitate the exploration of coherence between dimensions, we compare a high spatial coverage with 1250 camera positions to a lower coverage with 200 camera positions around the globe. The resulting image database contains 648750 (vs. 103800) images at 1200×1200 resolution, which add up to 359 GB (vs. 20.49 GB) of data. While this is larger than (or similar in size to) the original simulation run, it is much smaller than anticipated simulation sizes within the next few years.

To determine a good traversal order, we tested different traversal orders for 3 time steps. Despite very dense spatial coverage, this small number of time steps was sufficient to determine time as the dimension with strongest coherence, followed by φ and ϑ. Due to different colormaps used, the different variables are the least dominant dimension. We therefore encode the video files such that we first run through all time steps before switching to the next camera position, and cover each variable in a single block of the video.

2.2. Video Encoding

Video compression operates under the assumption that pairs of consecutive frames are similar. A video is composed of a series of images, or *frames*, which are played back at a specified frame rate, e.g. 25 frames per second (fps) in movies. At regular intervals (typically 5 seconds), a full freeze frame, or *keyframe* is stored. Between keyframes, there are *predicted frames*, which encode the differences to the previous and/or following frames using movement vectors and differencing. Using these predictions, one can achieve significant savings in storage [Ric04, Ric11]. Recent video codecs include H.264/AVC [Kal06], and the newer H.265 [SR14]. While H.265 generates higher quality videos at a smaller file size, this has a significant cost [GMM*13]. In a performance test, we found that H.264 only takes 59% as much time as H.265 to convert a series of images to a video file, and 45% as much time to extract a single frame. As interactive access is a concern for usability, we chose to use H.264, which is available across all platforms through the FFmpeg library [FD]. Video files are generated from a list of files using on-the-fly stream copy, the faster of two encoding options which yield identical results. We enable *fastdecode* for quick access to single frames, and we deactivate the audio channel to save space. On its own, video encoding is quasi-lossless [FD], but it provides compression through similarities between frames. Very minimal loss is caused by the application of Discrete Cosine Transform (DCT), as well as conversion from RGB colorspace to YUV colorspace.

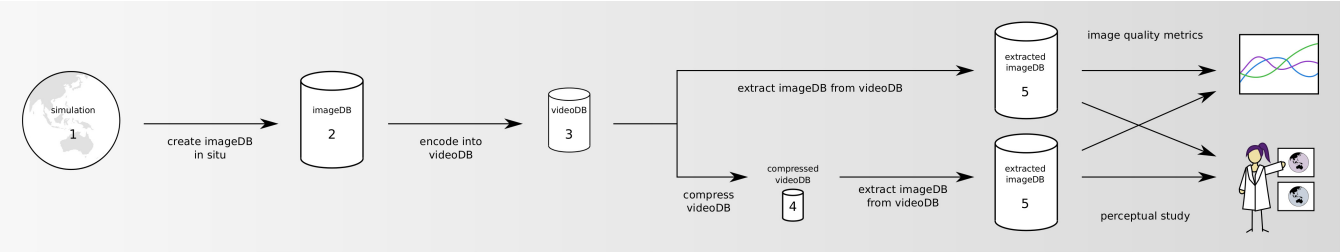

Figure 2: *Video compression workflow. During simulation (1), an image database (2) is written out in-situ . It is then encoded as a video file (3), which can be compressed in an optional step (4) and extracted again into images (5). The resulting images are evaluated based on image quality metrics, resulting database sizes and performance, as well as user studies to determine perceptual quality.*

2.3. Video Compression and Image Extraction

Additional compression can be achieved at the expense of lower image quality. Similar to JPEG, quantization can be employed to further compress the video file. Quantization is applied through setting a *Constant Rate Factor (CRF)* between 1 (lossless) and 51 (lossiest), where a CRF of 18 is considered "visually lossless" [FD]. The range is on an exponential scale: a difference of ± 6 corresponds to a change in file size by a factor of 2.

To get an overview of the data, it suffices to watch a video file with a low frame rate. However, if a user wants to interact with the data through a Cinema viewer [Dat17], specific frames need to be retrieved. To support this precise selection, direct access to specific frames of the video is needed. To find the correct frame, we generate a matrix storing indices for each parameter combination (variable, time, φ, ϑ). To obtain a frame, we use input seeking frame extraction, which skips ahead to the nearest keyframe and starts seeking from there, resulting in a very fast lookup [FD].

3. Analysis

For our analysis, we chose six regions (some of which are pictured in Fig. 3) with clearly identifiable eddies and currents, features of interest to climate scientists: the Agulhas Retroflection (AR) off the coast of South Africa, the Gulf Stream (GS), the Indian Ocean (IO), the Kuroshio Current (KC) along the coast of Japan, the North Pole (NP) and the South Pole (SP). These six regions vary in the amount of land versus ocean and in the size and type of currents and eddies.

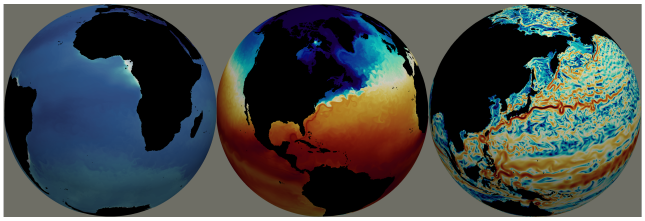

Figure 3: *Three of the regions used for analysis, from left to right: Agulhas Retroflection, Gulf Stream, and Kuroshio Current. The variables displayed, from left to right, are salinity (SA), temperature (TE), and kinetic energy (KE).*

3.1. Speed

There are two operations for which speed is critical: encoding and arbitrary access. For video codecs, the compression factor is not the only aspect that is affected by similarity between frames – similar frames are also faster to encode and compress. Creating all information required for video compression takes about 1.5 hours for the test database. However, if the parameters are known (time steps, φ, ϑ, variables), this can be computed and stored while the simulation is run. Reading this stored information back in only takes 0.07 seconds. Encoding a video takes about 1 hour, subsequently compressing it takes an average of 1-2 hours, depending on frame content, number of frames, and CRF. Arbitrary access to a single frame is faster if frames are similar because differences to keyframes are easier to compute. Extraction times for individual images fluctuate based on proximity to keyframes. The statistics described in the following are computed across all traversal methods and frame rates. For our example database, we extracted 13494 individual images from 4 video databases (encoded only, and compressed with CRFs 30, 34, and 51). Extraction times ranged from 247 to 337 ms, with both mean and median at 279 ms.

3.2. Compression

Thus far, we have described conversion of an image database to a video database using pure video encoding. However, as demonstrated in Figure 1, the perceptual quality is not negatively impacted. This assessment was confirmed through user evaluation, as described in Section 3.3. We compared compressed sizes for different traversal orders, varying the order of dataset variables, time, and space (φ, ϑ). For all traversals, we can see the same trend: database sizes drop with increasing frame rates. The most efficient traversal order (variable, time, space) requires less than half as much space as the least efficient order (time, variable, space). In addition to pure video encoding, we compressed video databases in a separate compression pass with a CRF in the range $[1, 51]$. For small CRF, file sizes are much larger than their original size, due to the fact that DCT is not efficient for this type of data. At a CRF of about 18, the compressed database reaches the original size.

Table 1 gives an overview of size reduction in comparison to both image databases across different steps of the workflow. All video databases listed are using optimal traversal at a frame rate of 30 fps. At 6.3 GB, the uncompressed large video database (1250 cameras) is 1.6 % the size of its image database, about two orders of

Table 1: *Comparison of compression for two databases with different numbers of "cameras" positioned around the globe.*

Database	1250 cameras		200 cameras	
	Size	% IDB	Size	% IDB
Image DB (IDB)	359 GB	100 %	20.49 GB	100 %
Video DB (VDB)	6.3 GB	1.6 %	2.0 GB	12.5 %
Video DB, CRF=30	2 GB	0.6 %	684 MB	4.2 %
Video DB, CRF=34	1.1GB	0.3 %	406 MB	2.5 %
Video DB, CRF=51	93.2 MB	0.03 %	50 MB	0.3 %

magnitude smaller. For the smaller video database (200 cameras), there is less spatial coherence between images from different perspectives, resulting in a decrease of one order of magnitude (12 %). Starting with the uncompressed video database, compression performance is similar. Using CRF=30, we reduce the database size further to 32 % of the video database. A compression of CRF=34 results in ca. 18 %, and at maximum compression (CRF=51), size drops to 0.02 % of the uncompressed video database. However, this comes at the cost of significant perceptual loss, as seen in Figure 1.

3.3. Perceptual Evaluation

In addition to the above error metrics, we must consider when a compressed image is no longer useful from the domain expert point of view. We asked two experts to evaluate representative compressed images, a Ph.D. climate scientist and a senior graduate student in Computer Science with expertise in feature identification w.r.t. ocean eddies. The experts agreed that the images became unusable at CRF=38. They transitioned to "marginally acceptable" between CRF=34 and CRF=36 and were deemed "completely usable" at CRF=30, with some slight variations based on the size and number of visible eddies and the amount of land in the image. In addition, the video compression images were used in a crowdsourced psychophysical evaluation as a use case for the Evaluation Toolkit [TBR17]. Using a classic two-alternative forced-choice (2AFC) approach [Fec89] with 282 crowdsourced subjects, the perceptual discrimination threshold was determined to be between CRF=34 and CRF=36, in agreement with expert opinion.

3.4. Quantitative Evaluation

We assess computational quality and accuracy based on the color-adjusted version of some common image metrics [CLS15, GL12]. The most relevant image quality metrics are Mean Absolute Error (MAE), Peak Absolute Error (PAE), Root Mean Square Error (RMSE), and Peak Signal-to-Noise Ratio (PSNR). For all images of the six regions and all time steps, we compare images extracted from compressed and uncompressed video databases with corresponding ones from the original image database.

As expected, the different errors rise with higher compression, whereas PSNR falls with higher compression. Errors also increase for higher frame rates as they have fewer keyframes and are therefore more prone to error propagation, and for less similar image sequences since more similar sequences enable a more precise differencing. Table 2 presents the median and average values for each of these metrics and different CRF settings. As can be seen, there

Table 2: *Comparison of error metrics of all images by compression rate over all images, and filtered by variable for CRF=30. All measurements are computed in comparison to an image from the original database, and they are given as median / mean.*

CRF	MAE	PAE	RMSE	PSNR
No CRF	0.008 / 0.024	0.79 / 0.67	0.03 / 0.05	80.1 / 78.6
CRF=30	0.009 / 0.025	0.78 / 0.68	0.02 / 0.05	80.2 / 78.3
CRF=34	0.009 / 0.025	0.76 / 0.68	0.03 / 0.05	80.2 / 77.9
CRF=51	0.018 / 0.033	0.84 / 0.83	0.04 / 0.06	77.1 / 74.2
KE	0.061 / 0.060	0.97 / 0.96	0.13 / 0.12	65.9 / 66.6
SA	0.005 / 0.005	0.26 / 0.32	0.01 / 0.01	87.8 / 87.8
TE	0.009 / 0.009	0.78 / 0.75	0.02 / 0.02	80.2 / 80.4

are only small differences between the purely encoded video and and the videos compressed with CRF=30/34. For CRF=51, there is a significant drop in quality across all metrics. Another observation worth noting is the differences between variables. Salinity (SA) outperforms the other two by far, since it is much more evenly colored and therefore easier to compress. Kinetic Energy (KE) is the most challenging to compress due to the many small details and sharp changes. Temperature (TE) has significant detail around strong currents, but also large areas of similar color, resulting in a performance between the other two.

4. Conclusion

We have presented a workflow for efficient compression of ocean simulation databases into video databases. The basis of our work was a 359 GB image database generated from a 173 time step simulation run. With pure video encoding, we reduced the size by two orders of magnitude, and we studied the effects of further compression by additional 1-2 orders of magnitude. Even at 2-3 orders of magnitude in reduction, neither domain experts nor crowdsourced subjects in a perceptual study could discern a difference between the original and the compressed images. For compression levels in the range of CRF=30 to CRF=34, the database has a size of 1-2 GB, small enough to share through cloud services or quickly download to a desktop computer. The smallest compression we were able to obtain through H.264 was 93.2 MB, about four orders of magnitude in reduction. However, the resulting image quality is well outside the acceptable range of quality loss.

In conclusion, we have found that video encoding and compression techniques make it possible to compress image databases efficiently and quickly (compared to the simulation run-time) to shareable sizes. Single images can be extracted in an average time of 279 ms, making video databases a good storage option for files. For even faster access, one can extract the full database onto the disk of a receiving computer.

Acknowledgments

This material is based upon work supported by Dr. Lucy Nowell of the U.S. Department of Energy Office of Science, Advanced Scientific Computing Research under Award Numbers DE-AS52-06NA25396 and DE-SC-0012516. The authors would like to thank Dr. Phillip Wolfram and Divya Banesh. This work was released under LA-UR-17-21590.

References

[ABG*15] AYACHIT U., BAUER A., GEVECI B., O'LEARY P., MORELAND K., FABIAN N., MAULDIN J.: ParaView Catalyst: Enabling in situ data analysis and visualization. In *Proceedings of the First Workshop on In Situ Infrastructures for Enabling Extreme-Scale Analysis and Visualization* (2015), ACM, pp. 25–29. 2

[AJO*14] AHRENS J., JOURDAIN S., O'LEARY P., PATCHETT J., ROGERS D. H., PETERSEN M.: An image-based approach to extreme scale in situ visualization and analysis. In *Proceedings of the International Conference for High Performance Computing, Networking, Storage and Analysis* (Piscataway, NJ, USA, 2014), SC '14, IEEE Press, pp. 424–434. 2

[ASW12] ATANASOV A., SRINIVASAN M., WEINZIERL T.: Query-driven parallel exploration of large datasets. In *Large Data Analysis and Visualization (LDAV), 2012 IEEE Symposium on* (2012), IEEE, pp. 23–30. 1

[BAB*12] BENNETT J. C., ABBASI H., BREMER P.-T., GROUT R., GYULASSY A., JIN T., KLASKY S., KOLLA H., PARASHAR M., PASCUCCI V., ET AL.: Combining in-situ and in-transit processing to enable extreme-scale scientific analysis. In *High Performance Computing, Networking, Storage and Analysis (SC), 2012 International Conference for* (2012), IEEE, pp. 1–9. 1

[CLS15] CELEBI M. E., LECCA M., SMOLKA B.: *Color Image and Video Enhancement*. Springer, 2015. 4

[Dat17] DATA VISUALIZATION AT SCALE TEAM: Cinema-science: Capture, store and explore extreme scale scientific data. http://www.cinemascience.org. Accessed: Feb 27, 2017, 2017. 2, 3

[EGH*06] ELLSWORTH D., GREEN B., HENZE C., MORAN P., SANDSTROM T.: Concurrent visualization in a production supercomputing environment. *Visualization and Computer Graphics, IEEE Transactions on 12*, 5 (2006), 997–1004. 2

[FD] FFMPEG-DEVELOPERS: FFmpeg and H.264 encoding guide. https://trac.ffmpeg.org/wiki/Encode/H.264. 2, 3

[Fec89] FECHNER G. T.: *Revision der Hauptpunkte der Psychophysik*, 2nd ed., vol. 2. Breitkopf & Härtel, Leipzig, 1889. 4

[FFSE14] FERNANDES O., FREY S., SADLO F., ERTL T.: Space-time volumetric depth images for in-situ visualization. In *Large Data Analysis and Visualization (LDAV), 2014 IEEE 4th Symposium on* (2014), IEEE, pp. 59–65. 2

[FMT*11] FABIAN N., MORELAND K., THOMPSON D., BAUER A. C., MARION P., GEVECI B., RASQUIN M., JAN K. E.: The ParaView coprocessing library: A scalable, general purpose in situ visualization library. In *Large Data Analysis and Visualization (LDAV), 2011 IEEE Symposium on* (2011), IEEE, pp. 89–96. 2

[GABJ08] GOSINK L. J., ANDERSON J. C., BETHEL E., JOY K. I.: Query-driven visualization of time-varying adaptive mesh refinement data. *Visualization and Computer Graphics, IEEE Transactions on 14*, 6 (2008), 1715–1722. 1

[GL12] GUNTURK B. K., LI X.: *Image restoration: fundamentals and advances*. CRC Press, 2012. 4

[GMM*13] GROIS D., MARPE D., MULAYOFF A., ITZHAKY B., HADAR O.: Performance comparison of H. 265/MPEG-HEVC, VP9, and H. 264/MPEG-AVC encoders. In *Picture Coding Symposium (PCS), 2013* (2013), IEEE, pp. 394–397. 2

[GS01] GUTHE S., STRASSER W.: Real-time decompression and visualization of animated volume data. In *Visualization, 2001. VIS'01. Proceedings* (2001), IEEE, pp. 349–572. 2

[Kal06] KALVA H.: The H.264 video coding standard. *IEEE Computer Society 13* (2006), 86–90. 2

[KY14] KAGEYAMA A., YAMADA T.: An approach to exascale visualization: Interactive viewing of in-situ visualization. *Computer Physics Communications 185*, 1 (2014), 79–85. 2

[LI06] LINDSTROM P., ISENBURG M.: Fast and efficient compression of floating-point data. *Visualization and Computer Graphics, IEEE Transactions on 12*, 5 (2006), 1245–1250. 1

[Lin14] LINDSTROM P.: Fixed-rate compressed floating-point arrays. *Visualization and Computer Graphics, IEEE Transactions on 20*, 12 (2014), 2674–2683. 1

[LJ14] LEHMANN H., JUNG B.-I.: In-situ multi-resolution and temporal data compression for visual exploration of large-scale scientific simulations. In *Large Data Analysis and Visualization (LDAV), 2014 IEEE 4th Symposium on* (2014), IEEE, pp. 51–58. 1

[MJM13] MUNDAY D. R., JOHNSON H. L., MARSHALL D. P.: Eddy Saturation of Equilibrated Circumpolar Currents. *Journal of Physical Oceanography 43* (Mar. 2013), 507–532. 1

[MM05] MALTRUD M., MCCLEAN J. L.: An eddy resolving global 1/10° ocean simulation. *Ocean Modelling 8*, 1-2 (2005), 31–54. 2

[MOD15] METERE A., OPPELSTRUP T., DZUGUTOV M.: A new computer program for topological, visual analysis of 3D particle configurations based on visual representation of radial distribution function peaks as bonds. *arXiv preprint arXiv:1503.04449* (2015). 2

[MPA] Model for Prediction Across Scales (MPAS) website. http://mpas-dev.github.io/. 2

[NWP*14] NOUANESENGSY B., WOODRING J., PATCHETT J., MYERS K., AHRENS J.: ADR visualization: A generalized framework for ranking large-scale scientific data using analysis-driven refinement. In *Large Data Analysis and Visualization (LDAV), 2014 IEEE 4th Symposium on* (2014), IEEE, pp. 43–50. 1

[Ric04] RICHARDSON I. E.: *H. 264 and MPEG-4 video compression: video coding for next-generation multimedia*. John Wiley & Sons, 2004. 2

[Ric11] RICHARDSON I. E.: *The H. 264 advanced video compression standard*. John Wiley & Sons, 2011. 2

[RPH*13] RINGLER T., PETERSEN M., HIGDON R. L., JACOBSEN D., JONES P. W., MALTRUD M.: A multi-resolution approach to global ocean modeling. *Ocean Modelling 69* (2013), 211 – 232. 2

[SBS04] SOHN B.-S., BAJAJ C., SIDDAVANAHALLI V.: Volumetric video compression for interactive playback. *Computer Vision and Image Understanding 96*, 3 (2004), 435–452. 2

[SPA*15] SAMSEL F., PETERSEN M., ABRAM G., TURTON T., ROGERS D., AHRENS J.: Visualization of ocean currents and eddies in a high-resolution global ocean-climate model. In *Proceedings of the International Conference on High Performance Computing, Networking, Storage and Analysis* (2015), no. 11. 1

[SR14] SEELING P., REISSLEIN M.: Video traffic characteristics of modern encoding standards: H. 264/AVC with SVC and MVC extensions and H. 265/HEVC. *The Scientific World Journal 2014* (2014). 2

[TBR17] TURTON T. L., BERRES A. S., ROGERS D. H.: ETK: An evaluation toolkit for visualization user studies, June 2017. Accepted into EuroVis 2017: 19th EG/VGTC Conference on Visualization. 4

[WCBP12] WIDANAGAMAACHCHI W., CHRISTENSEN C., BREMER P.-T., PASCUCCI V.: Interactive exploration of large-scale time-varying data using dynamic tracking graphs. In *Large data analysis and visualization (LDAV), 2012 IEEE Symposium on* (2012), IEEE, pp. 9–17. 1

[WMB*11] WOODRING J., MNISZEWSKI S., BRISLAWN C., DEMARLE D., AHRENS J.: Revisiting wavelet compression for large-scale climate data using JPEG 2000 and ensuring data precision. In *Large Data Analysis and Visualization (LDAV), 2011 IEEE Symposium on* (2011), IEEE, pp. 31–38. 2

[WPS*16] WOODRING J., PETERSEN M., SCHMEISSER A., PATCHETT J., AHRENS J., HAGEN H.: In situ eddy analysis in a high-resolution ocean climate model. *Visualization and Computer Graphics, IEEE Transactions on 22*, 1 (Jan 2016), 857–866. 1